**Nationaal Lucht- en Ruimtevaartlaboratorium**
National Aerospace Laboratory NLR


NLR-TP-98423

# Advances in the modelling of cracks and their behaviour in space structures

A.U. de Koning, H.J. ten Hoeve, F.P. Grooteman and C.J. Lof

**Nationaal Lucht- en Ruimtevaartlaboratorium**

National Aerospace Laboratory NLR


NLR-TP-98423

# Advances in the modelling of cracks and their behaviour in space structures

A.U. de Koning, H.J. ten Hoeve, F.P. Grooteman and C.J. Lof

This report is based on a presentation to be held on the European Conference of Spacecraft Structures, Materials and Mechanical Testing, 4-6 November 1998, Braunschweig, Germany.



| | |
|---|---|
| Division: | Structures and Materials |
| Completed: | 5 October 1998 |
| Classification of title: | Unclassified |

## Contents



(8 pages in total)

# ADVANCES IN THE MODELLING OF CRACKS AND THEIR BEHAVIOUR IN SPACE STRUCTURES

A.U. de Koning, H.J. ten Hoeve, F.P. Grooteman and C.J. Lof

National Aerospace Laboratory, NLR
P.O.Box 153, 8300 AD Emmeloord
The Netherlands
E-mail: akoning@nlr.nl

## ABSTRACT

In damage tolerance analyses of cracked space structures, the stress intensity factor (SIF) distribution along the crack front plays an important role. Nowadays, 3D-finite element analysis methods have been developed to a level that allows determination of stress intensity factor distributions for cracks in complicated structural parts such as bolt - nut assemblies and bars loaded in tension and bending. Recently, some new stress intensity solutions were obtained for new and existing configurations. These cases will be discussed.

A second important improvement in the description of crack growth behaviour is the introduction of a discretized STRIP-YIELD model for simulation of plasticity effects near a crack front and in the wake of a growing crack. The model allows a description of plasticity induced crack closure in fatigue loaded components. The model was implemented in the NASGRO (ESACRACK) crack growth analysis software, and the results of recent verifications by comparing predicted results with data obtained experimentally, will be discussed.

It is important to note that the STRIP-YIELD model can be used to calculate values for a variety of fracture mechanics parameters such as the Crack Tip Opening Angle (CTOA), J-integral, Crack Tip Opening Displacement (CTOD), Crack Tip Strain Rate, etc. These parameters can be used to formulate more accurate and physically sound crack growth laws. An example will be given.

**Key words**: Crack growth equations, Stress intensity factors, Strip Yield model, Static crack growth.

## 1. INTRODUCTION

Crack growth calculations are usually carried out on the basis of the stress intensity factor. This linear elastic property characterises the state of stress near the crack tip. A crack growth equation relates the crack growth rate to the stress intensity factor range ($K_{max}$ - $K_{min}$). Basically, a crack growth calculation involves integration of the crack growth rate equation over all cycles in the load history.

Computer programs for prediction of crack growth usually include a database of stress intensity factors for geometries commonly used. The stress intensity factors in these databases are obtained from analytical solutions or from FEM or BEM calculations. In the latter cases the program interpolates between given solutions. From the modelling point of view the BEM solutions are easier to obtain. However, with modern techniques, FEM solutions can be obtained easily too in combination with sophisticated modelling options such as gap elements and tyings. In such applications automated mesh generation should be based on a parameterised description of the geometry and the use of automated pre-processing software to include gap elements, tyings and singular crack front elements, is inevitable. Further, postprocessor programmes became available for computation of stress intensity factors from the results of the FEM analyses. Recently, some of the stress intensity factor solutions obtained using the software described above were included in a version of the NASGRO (ESACRACK) software for damage tolerance analyses. This software is sometimes referred to as NASA/FLAGRO. These cases will be discussed in section 2.

The fatigue crack growth rate equation in its simplest form, called the Paris equation, describes the logarithmic crack growth rate as a linear function of the logarithmic stress intensity factor range. The constants in this equation, are obtained from a fit to experimental data. It is known that these constants are different for different stress ratio's. Elber[1] showed that this stress ratio effect is the result of local plastic deformations near the crack tip. The same effect turned out to be responsible for plasticity induced retardation and acceleration of crack growth. An important improvement in the description of crack growth behaviour was the introduction of a discretized STRIP-YIELD model for simulation of these plasticity effects

near a crack front and in the wake of a growing crack. The model was implemented in the NASGRO (ESACRACK) software and the results of recent verifications, by comparing predicted results with data obtained experimentally, will be discussed in section 3.

It is known from experiments, that for small, as well as for large values of the stress intensity factor range, the growth rate deviates from the linear description given by the Paris equation. In the NASGRO (ESACRACK) software a modified Paris equation is used to describe this deviation called NKHF or NASGRO2.0 equation. This is an empirical modification of the Paris equation. In 1994 a physically based modification of the Paris equation was proposed[2] and implemented in the NASGRO software. This equation is referred to as ESA/NLR equation. The development of this equation is being continued at NLR, based on the notion that the STRIP-YIELD model can be used to calculate values for a variety of fracture mechanics parameters such as the Crack Tip Opening Angle (CTOA), J-integral, Crack Tip Opening Displacement (CTOD), Crack Tip Strain Rate, etc. This allows a detailed study of the behaviour of such parameters in relation to the applied load and variations in the applied load. It will be shown that the better understanding of the deformation processes near the crack front can be used to formulate more accurate and physically more sound, crack growth laws.

## 2. STRESS INTENSITY SOLUTIONS

Recently, stress intensity factors were obtained from finite element solutions for the following configurations:

- bolt - nut assembly[3]
- lap joint[4]
- rectangular bar[5]

The stress intensity factors for the bolt - nut assembly are included in the NASGRO or ESACRACK software as cases SC20 till SC25. The solutions for the cracks in a rectangular bar are used to derive parameters for the weight functions used to calculate stress intensity factors for any loading system on this geometry. All stress intensity values were calculated from the linear solution obtained with MARC using the virtual crack extension (VCE) method as well as the crack tip opening (COD) displacement extrapolation method[6].

### 2.1 BOLT - NUT ASSEMBLY

A full 3D finite element model of the bolt - nut assembly was developed. The thread is modelled as a helical surface. In the model of the nut the runout of the thread is modelled in 3D and rigidly coupled to one side of the bolt thread. Over 7000 higher order isoparametric (20 node) brick elements are used to model the bolt and nut. The crack tip was modelled with crack tip elements which describe the $1/\sqrt{r}$ singularity in the stress field. In all analyses the bolt material used is: Ti-6Al-4V ($E$ = 10000 MPa, $\nu$ = 0.33) combined with a steel nut (($E$ = 210000 MPa, $\nu$ = 0.33). The model is presented in figure 1.

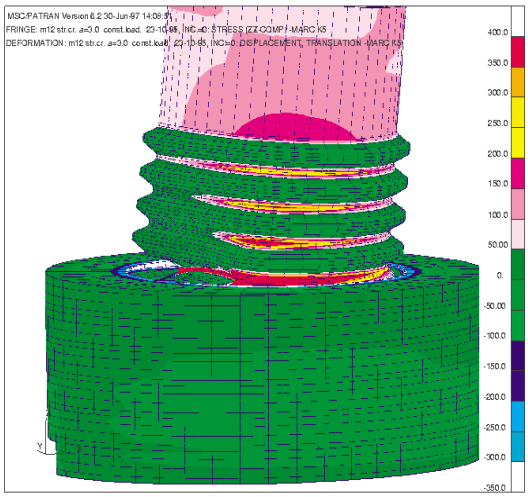

**Figure 1:** Finite element model of a bolt - nut assembly.

A total of 28 finite element analyses were carried out: 16 with an applied tensile load and 12 with an applied bending load. The 16 calculations carried out with a tensile load include 12 calculations for M12*1.25 thread with different crack sizes and shapes and 4 for M8*1.0 thread (one crack shape and different crack sizes). For the bending load only M12*1.25 thread cases were analysed. In table 1 all cases analysed are given.

| e | crack shape | crack size [mm] | loading |
|---|---|---|---|
| M12*1.25 | straight | 0.68 | tension + bending |
| | | 1.50 | tension + bending |
| | | 3.00 | tension + bending |
| | | 4.67 | tension + bending |
| | a/c = 0.645 | 1.06 | tension + bending |
| | | 2.40 | tension + bending |
| | | 3.60 | tension + bending |
| | | 4.80 | tension + bending |
| | a/c = 1.0 | 1.20 | tension + bending |
| | | 2.05 | tension + bending |
| | | 3.55 | tension + bending |
| | | 4.60 | tension + bending |
| M8*1.0 | a/c = 0.645 | 0.90 | tension |
| | | 1.50 | tension |
| | | 2.29 | tension |
| | | 3.15 | tension |

**Table 1**: Matrix of analysed cases used to derive a table for stress intensity solutions for metric bolt/nut assemblies (a/c = crack aspect ratio).

At NLR, the numerical results were verified by comparison with stress intensity factor solutions derived from markings on the fracture surface of specimen tested.

From the results of the finite element calculations a data table was generated and included in the NASGRO (ESACRACK) software. This table is used to determine stress intensity solutions for other types of metric fine thread using a linear interpolation or extrapolation scheme.

## 2.2 LAP JOINT

A lap joint configuration with three rivet rows has been modelled. The FEM model contains two lapped plate strips. The width of these strips is equal to half the rivet pitch. A symmetry condition is applied to the plane through both rivets. The lateral plane through the centre of the second of the three rivets has been considered as a plane of anti symmetry.

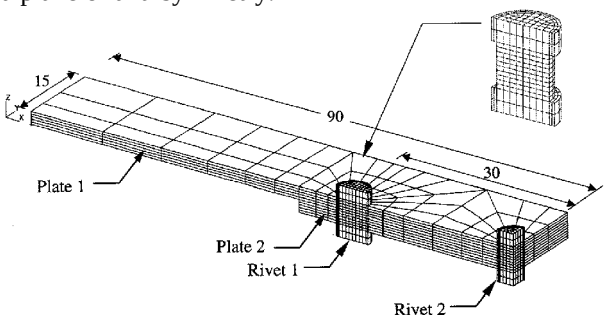


**Figure 2:** Finite Element Model of a lap joint

The plate thickness is 2 mm, and the width is 15 mm. The rivets were modelled “neat fit” in the 5 mm holes. Contact between plates and rivet shanks has been modelled using “gap”-elements. Friction has not been taken into account. Contact between the plates was modelled via tying of nodes between both plates in a restricted area around the rivets. Also, rivet head nodes have been tied to corresponding nodes in the plate. This tying was applied only to the normal degrees of freedom (z-direction). Plates and rivet heads may shift independently in the loading direction. The influence of the residual stresses due to the riveting process were simulated by heating the rivets until a 1% radial expansion was obtained. Axial shrink, to an amount of 0.5 percent strain, was obtained by selecting a proper coefficient of thermal expansion for the axial direction. This represents a high squeeze force (HSF). A low squeeze force (LSF) was modelled by selecting a coefficient of thermal expansion that gave no axial strain. A 0.8 mm quarter circular corner crack was modelled at the hole edge of rivet 1. The stress intensity factors for this configuration loaded with a remote tensile stress of 100 MPa were calculated using the virtual crack extension method. The results are given in table 2 together with the values obtained from the Newman/Raju solution. For the latter solution the bypass load and bending stress are calculated using industry standard handbook equations.

| Solution | K [MPa√m] |
|---|---|
| Newman/Raju | 10.24 |
| LSF | 11.68 |
| HSF | 3.95 |

**Table 2**: Comparison of stress intensity factors for a lap joint.

From this table it can be concluded[4] that a high squeeze force will result in a longer crack growth life. This was shown experimentally by Müller[7].

## 2.3 RECTANGULAR BAR

In order to be able to calculate stress intensity factors for a given geometry and an arbitrary loading system the weight function technique can be utilised[8]. In order to derive parameters of the weight functions, stress intensity factor solutions have to be available for simple loading systems, such as: uniform and linear distributed loads over the crack surface. Furthermore, complex loading systems have to be available in order to be able to validate the derived weight functions e.g.: a quadratic stress distribution over the crack surface. For a quarter elliptical corner crack in a bar or plate, stress intensity solutions are available for $0.2 \leq a/c \leq 1.0$. However for practical applications reliable results for $a/c = 0.1$ are required. Therefore, stress intensity factor solutions have been calculated from finite element analysis for $a/c = 0.1$ and a number of crack sizes (a/t and c/w) and different loading systems. In case of half elliptical surface cracks, stress intensity factor solutions are lacking for in plane bending loads. The stress intensity factors are normalised according to:

$$Y = \frac{K_I}{\sigma_0 \sqrt{\pi a}}$$

Where: $K_I$ the mode I stress intensity factor, $\sigma_0$ the peak stress applied and a the crack depth. In figure 3, the calculated normalised stress intensity factor for a corner crack in a bar or plate is compared with the values obtained with NASGRO. The latter are extrapolated from FEM solutions obtained by Raju and Newman[9]. The dimensionless co-ordinate $S/S_0$ runs from –1 to 1 starting at the crack tip on the surface (c).

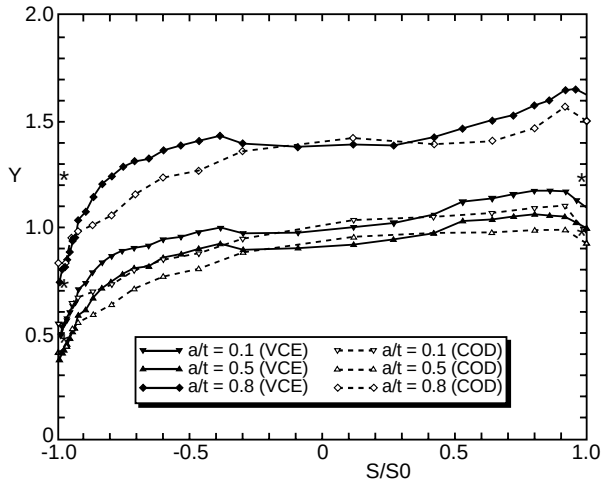


**Figure 3:** Normalised stress intensity factor for a corner crack in a bar subjected to remote bending (a/c=1.0, c/w=0.8). Drawn lines: VCE method; dotted lines: COD method; *: NASGRO result.

Figure 4 shows the normalised stress intensity factor for a surface crack in a plate loaded with an in plane bending moment.

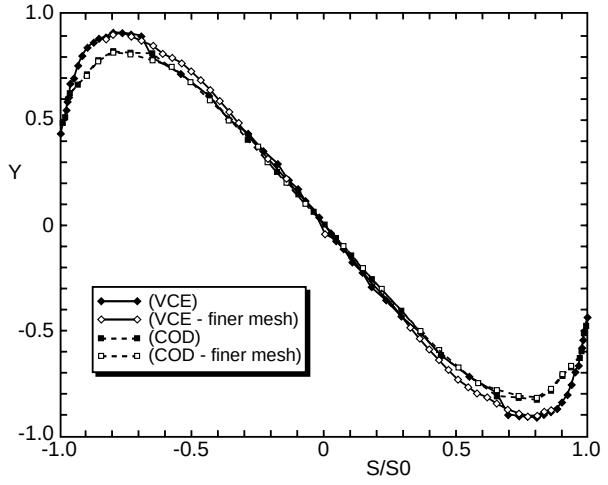


**Figure 4:** Normalised stress intensity factor for a surface crack subjected to remote bending (a/c=1.0, c/t=0.8 and a/w=0.8). Drawn lines: VCE method; dotted lines: COD method.

These stress intensity factor solutions will be used to improve the solutions in the NASGRO or ESACRACK database for CC01, SC01 and SC02.

## 3. STRIP YIELD MODEL

In the open literature[10,11] and other documents[12,13] the Strip Yield model is discussed extensively. Results obtained using different implementations of the model (NASA-FASTRAN and ESA/NLR-NASGRO or ESA-CRACK) were compared and it was concluded that the programs predict the same crack opening behaviour if the constraint effects on yielding are modelled in the same way. Nowadays, it is still hardly possible to investigate the constraint behaviour numerically. For primary plastic flow, full non-linear finite element calculations for investigation of the constraint behaviour were reported[14]. However, to the authors' knowledge, accurate results of such calculations are not available for secondary plasticity. Therefore, it is common practice to use experimental results to develop the constraint model. Based on an experimental program carried out recently[15], the constraint model for the wake of the crack was improved. These improvements are incorporated in the NASGRO or ESACRACK software.

In the present version of the software the constraint model is described using a constraint parameter $\alpha(\rho)$, which relates the yield stress in the Strip Yield elements $\sigma_{yld}$ to the uni-axial yield limit of the material $\sigma_{yd}$:

$$\sigma_{yd} = \alpha(\rho)\sigma_{yld}$$

The parameter $\rho$ indicates the positions in the plastic zone: $\rho = 0$ corresponds to the crack tip and $\rho = 1$ to the end of the plastic zone. To define the constraint parameter $\alpha(\rho)$ the following regimes are distinguished:

1. Primary plastic flow in tension
2. Secondary plastic flow in tension
3. Plastic flow in compression ahead of the tip
4. Plastic flow in compression in the wake of the crack

A full description of the constraint model for these regimes can be found in reference 13.

## 4. A NEW CRACK GROWTH RATE EQUATION

Usually, fatigue crack growth is assumed to occur in the upward part of a load cycle. In this part different regimes can be distinguished, depending on the loading history and the state of opening of the crack. To illustrate these domains, the loading path is shown in a stress intensity factor, K, versus crack size, c, plot in figure 5. The different loading regimes are indicated and discussed next.

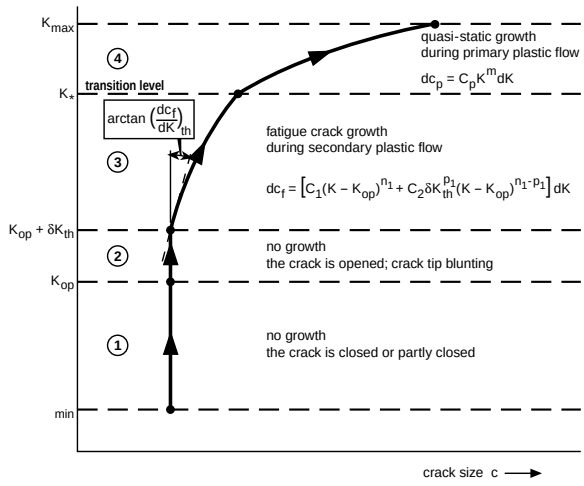


**Figure 5:** Regimes distinguished during the growth of one load cycle.

### 4.1 CLOSED CRACK REGIME 1, $K_{MIN} \le K < K_{OP}$

Starting at the intensity factor at the minimum load $K_{min}$ the load is increased until the crack opening level $K_{op}$ is attained. In this regime 1, characterised by $K_{min} < K < K_{op}$, the crack is at least partly closed and the contact areas on the crack surfaces decrease when the applied load is increased. Although the stress intensity factors in this regime are calculated assuming the presence of the crack, it is clear that the effective loading of the crack tip region is very small and no crack growth is assumed in this regime.

### 4.2 OPENED CRACK BUT NO GROWTH REGIME 2, $K_{OP} \le K < K_{OP} + \delta K_{TH}$

At level $K_{op}$ the crack is fully opened, but it takes another increase by $\delta K_{th}$ to initiate crack growth. Obviously, some crack tip blunting occurs in this regime. Models and empirical equations for computation of values for $K_{op}$ and $\delta k_{th}$ are discussed in reference 2.

### 4.3 FATIGUE CRACK GROWTH IN REGIME 3, $K_{OP} + \delta K_{TH} \le K < K_*$

Upon a further increase of the applied load, crack growth is initiated when the stress intensity factor K exceeds the level $K_{op} + \delta K_{th}$ In this regime 3, plastic deformations take place in a relatively small part of the plastic zone created by application of $K_{max}$ in a previous load cycle. At the load level $K = K_*$ primary plastic flow in virgin material reinitiates and the zone of material that actually is loaded to the yield limit is extending beyond the previous plastic zone.

### 4.4 QUASI-STATIC CRACK EXTENSION REGIME 4, $K_* \le K < K_{MAX}$

Loading above the transition level $K_*$ is assumed to induce quasi-static crack extension. In this regime the plastic deformation behaviour takes place under monotonic increasing loads. This implies that the effects of secondary cyclic loading on the actual material behaviour are lost. Thus, the crack opening load and threshold behaviour become insignificant. Moreover, the plastic zone sizes are much larger. To describe crack growth in this domain, the incremental formulation of the R (or J) curve approach is adopted.

### 4.5 TIME DEPENDENT LOADING, THRESHOLD AND FREQUENCY EFFECTS IN CORROSION FATIGUE

In reference 17 it is stated that the strain rate at the crack tip controls the crack growth process in a corrosive environment. This is based on the notion that there is a competition between the strain rate at the crack tip and the velocity of build-up of a passivating film, shielding the base metallic material at the crack tip from direct contact with the environment. If such a process is taking place, then strain rates larger than the overall build-up rate will allow direct contact (and attack) of the environment on the base metal of the alloy under consideration. This condition was used to formulate a criterion for initiation of accelerated fatigue crack growth due to this specific form of corrosion. It is assumed that, for this specific material/environment system, crack growth acceleration initiates when a certain threshold strain rate $\varepsilon_{th}$ is exceeded. This criterion can be used to calculate the lower bounds $t_i$ of the periods of time $t_i < t < t_e$ during which environmentally induced crack growth acceleration occurs. Once accelerated fatigue crack growth has initiated, the crack growth rate increases. In general, the crack growth rate becomes so high that direct contact between the environment and the base metal is self-contained. To stop it, the load must be brought to a hold or decreased. This implies that the period of accelerated growth ends close to the moment $t_m$ of application of the maximum load, that is $t_e = t_m$.
Values for $t_i$ and $t_m$ are used, respectively, as lower and upper bounds for integration of the time dependent part of the incremental corrosion fatigue crack growth law. This is discussed in detail in reference 17.

## 5. CONCLUSIONS

1. Progress has been made in automated parameterised FEM mesh generation, which includes contact analysis and other non-linear effects. A large number of complicated 3D FEM analysis can be executed efficiently and the

computation of K factor solutions can be done in an automated way.

2. The discretized Strip Yield model for computation of the plasticity induced crack opening levels has reached a level of efficiency and accuracy that it can be used in an industrial environment. By now, the constraint effects are modelled in agreement with results of non-linear 3D FEM analysis.
3. The incremental formulation of fatigue crack growth has opened new ways for inclusion of time dependent effects such as corrosion fatigue. In practice, other parameters (temperature, creep, etc) can be included in a similar way as demonstrated for corrosion fatigue crack growth.

## 6. ACKNOWLEDGEMENT

The research work described in this paper was executed under separate contracts with the Netherlands Agency for Aerospace programs (NIVR) and the European Space Agency (ESA).

## 7. REFERENCES

1. Elber, W., The Significance of Fatigue Crack Closure, ASTM STP 486, 1971, pp. 230-242.
2. Koning, A.U. de, Henriksen, T.K., Hoeve, H.J. ten, Recent Advances in the Modelling of Fatigue Crack Growth, NLR TP 94152 L.
3. Koning, A.U. de, Lof, C.J., Schra, L. Assessment of 3D stress intensity factor distributions for nut supported threaded rods and bolt/nut assemblies. NLR CR 96692 L.
4. Fawaz, F.A. Fatigue Crack Growth in Riveted Joints, Thesis, Delft, 1997.
5. Grooteman, F.P., Lof. C.J., Stress Intensity Factors for Corner and Surface Cracks in a Rectangular Bar. NLR CR 98254.
6. Bakker, A., The Three-dimensional J-integral, Thesis, Delft, 1984.
7. Müller, R.P.G., An Experimental and Analytical Investigation on the Fatigue Behaviour of Fuselage Riveted Lap Joints, The Significance of the Rivet Squeeze Force, and a Comparison of 2024-T3 and Glare 3, Thesis, Delft, 1995.
8. Wu, X.R., Carlsson, A.J., Weight Functions and Stress Intensity Factor Solutions, Pergamon Press, Oxford, 1991.
9. Raju, I.S., Newman, J.C. Jr., Stress Intensity Factors for Corner Cracks in Rectangular Bars, ASTM STP 969, 1988, pp.43-55.
10. Newman, J.C. Jr., A Crack Closure Model for Predicting Fatigue Crack Growth Under Aircraft Spectrum Loading, ASTM STP 748, 1981, pp. 53-84.
11. Koning, A.U. de, Liefting, G., Analysis of Crack Opening Behaviour by Application of a Discretised Strip Yield model, ASTM STP 982, 1988, pp. 437-458.
12. Newman, J.C. Jr., FASTRAN-II a Fatigue Crack Growth Structural Analysis Program, NASA TM 104159, 1992.
13. Koning, A.U. de, Hoeve, H.J. ten, User Manual for the Stripyntv2.0 Strip Yield Model in the NASGRO or ESACRACK software, NLR CR 97543 L.
14. Lof, C.J., Koning, A.U., 3-D FEM Analysis of Stresses and Deformations near the Crack Front of a Through Crack Growing under Fatigue Loading Conditions., NLR CR 96293 L.
15. Koning, A.U. de, Hoeve ten H.J., The Application of the Strip Yield Model in the Prediction of Fatigue Crack Growth., NLR CR 98057.
16. Hoeve, H.J. ten, Koning, A.U. de, User Manual for the Crack Opening Models in the Nasgro-Stripy-95 Program, NLR CR 95399 L.
17. Koning, A.U. de, Hoeve, H.J. ten, Henriksen, T.K., The Description of Crack Growth on the Basis of the Strip Yield Model for the Computation of Crack Opening Loads, the Crack Tip Stretch and Strain Rates, NLR TP 97511 L.